4.5   **OBSERVATIONS OF A NON-SUPERCELL TORNADIC THUNDERSTORM**
FROM A TERMINAL DOPPLER WEATHER RADAR

Justin D. Lane[*] and Patrick D. Moore
NOAA/National Weather Service
Greer, SC

1. INTRODUCTION

Despite numerous advances in meteorologists' understanding of severe weather and the innovations in technology that have occurred over the past 20 years, detection of non-supercell tornadoes (NST) continues to present a difficult challenge to operational forecasters. By definition, these tornadoes are not associated with mesocyclones (i.e., they do not develop in the "top-down" sequence).   The tornadic vortex is often too small or shallow to be resolved by the beam from the Weather Service Radar 1988 Doppler (WSR-88D), rendering the data from the Doppler velocity moment inconclusive in detection of NSTs. As a result, some events occur with little or no lead time. An informal study of tornado occurrence within the Greer, SC (GSP) county warning area from July 1995 through August 2006 found that approximately 43%[1] of tornadoes are not associated with deep, persistent mesocyclones. Although most NSTs are weak (F0 or F1), strong NSTs have been known to occur over the Carolinas (Lee and Jones 1998; McAvoy et al. 2000). An understanding of NSTs remains an important goal due to their relative frequency across the western Carolinas and the significant attention to them from NWS stakeholders across the region.

On 13 January 2006 at approximately 0110 UTC, an F1 tornado occurred within a shallow, quasi-linear convective system (QLCS) near Bessemer City (BC), NC (Fig. 1). The BC tornado developed within an environment characterized by strong shear (especially in the 0-3 km layer), weak buoyancy, and strong synoptic-scale forcing. Previous studies have documented cool-season NSTs developing within similar environments (McAvoy et al. 2000; Grumm and Glazewski 2004). These studies identified a characteristic radar reflectivity

---

[*]Corresponding author address: Justin Lane
1549 GSP Dr, Greer, SC 29651
e-mail: Justin.Lane@noaa.gov

[1] This study did not include tornadoes associated with tropical cyclones.

signature associated with shallow QLCSs whereby a fracture develops within the reflectivity field across a bowing segment associated with a line echo wave pattern (LEWP). This signature, often referred to as the "broken-S," develops prior to or concurrently with tornadogenesis.

Figure 1. Location of the Bessemer City tornado with respect to the Charlotte TDWR. Heavy black line marked by red flag just east of Bessemer City is the tornado track. Blue pin north/northwest of Charlotte is the location of the TDWR. The distance between these locations is 33 km.

The BC tornado occurred within close proximity (33 km) of the Terminal Doppler Weather Radar (TDWR) located near Charlotte, NC (TCLT). Examination of reflectivity data from TCLT and from the WSR-88D at Greer, SC (KGSP) revealed features similar to previous NST events associated with the "broken-S" signature. However, the data from the 5-cm TDWR provided much better detail of the structure of the tornadic QLCS, partially due to its proximity to the storm. (KGSP is located approximately 99 km from the storm location.) In addition, the higher resolution data from the 5-cm radar provided a unique opportunity to analyze the structure of a tornadic QLCS in an operational setting. Analysis of this structure indicated that a rear-to-front, descending air current may have played an important role in tornadogenesis.

2. ENVIRONMENT

A highly amplified, progressive mid and upper level trough moved across the Mississippi Valley during the day on 13 January, with the axis of the 500 hPa trough reaching the Tennessee Valley by 0000 UTC on 14 January (not shown). Deep synoptic scale forcing, associated with the left exit region of a jet streak moving over the

northern Gulf Coast at 300 hPa (not shown) and diffluent flow in advance of the mid level trough, spread a large area of stratiform precipitation with embedded convection across the western Carolinas in the mid-afternoon. However, by late afternoon, a dry slot wrapping around the 500 hPa low (Fig. 2) resulted in a reduction in precipitation coverage across Upstate South Carolina. Numerous studies have documented the important role of mid-level dry air advection, into a strongly sheared and weakly buoyant environment, in enhancing tornado potential, particularly in tropical environments (Curtis 2004).
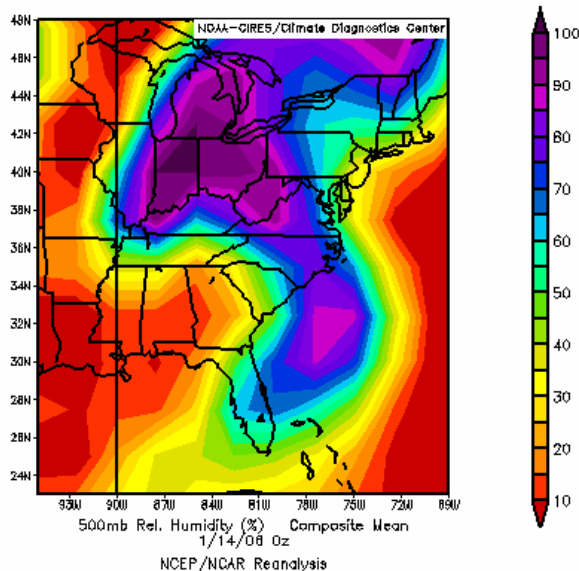

Figure 2. NCEP reanalysis of 500 hPa relative humidity at 0000 UTC 14 January.

Across the Piedmont, a low level jet at 850 hPa associated with the thermally indirect circulation in the exit region of the approaching jet streak strengthened to approximately 30 m s^{-1}, while the winds at that level backed in response to the approaching short wave (not shown). An upper air sounding taken at Greensboro, North Carolina (GSO), at 0000 UTC on 14 January (Fig. 3) revealed the presence of strong shear in the 0-6 km layer. Storm relative helicity in the 0-1 km layer was 283 m^2 s^{-2}, well above the median value of 0-1 km SRH of 137 m^2 s^{-2} found to be associated with weak tornadoes (Thompson et al. 2003). The sounding also showed relatively weak buoyancy for a surface-based parcel in spite of the unusually warm and moist air mass across the Piedmont of the Carolinas, characterized by temperatures in the lower 60s and dew points in the upper 50s ahead of the surface cold front (not shown).

However, a steeper lapse rate in the 850-700 hPa layer provided 198 J kg^{-1} of Convective Available Potential Energy.
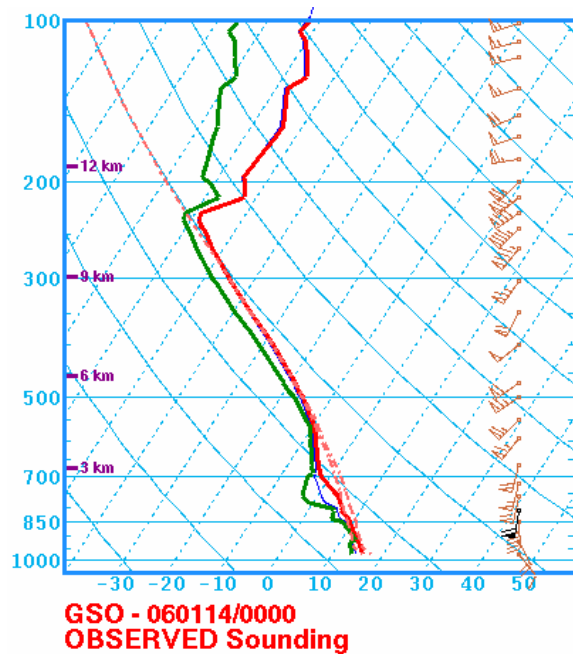

GSO - 060114/0000
OBSERVED Sounding

Figure 3. SkewT - log P diagram of upper air sounding from GSO at 0000 UTC 14 January. The low level wind maximum at 800 mb is highlighted in black.

3. CONVECTIVE EVOLUTION

A line of convection began to intensify between 2100 and 2130 UTC along the back edge of the deep forcing (coincident with the cold front) across northeast Georgia, probably aided by the steeper mid-level lapse rates that developed due to the advection of drier mid-level air (not shown). The convection continued to intensify and organize as it moved into northern South Carolina around 2200 UTC (not shown). Data from KGSP indicated several LEWPs developed within this QLCS as it moved across Upstate South Carolina, some of which evolved into "broken-S" signatures. The strongest of these signatures is shown in Fig. 4. However, this particular signature was apparently not associated with a tornado on 13 January 2006.

By 0047 UTC, the QLCS had moved within range of TCLT. At this time, the 0.2 degree base reflectivity image (Fig. 5) from TCLT indicated another "broken-S" signature in progress approximately 60 km southwest of the radar. By 0059 UTC, the reflectivity between the northern and southern segment continued to weaken,

while the southern segment had pushed out slightly ahead of the northern (Fig. 6). This was approximately 10 minutes prior to tornado occurrence near Bessemer City. The 0.2 degree radial velocity image from TCLT at this time (Fig. 7, storm relative velocity was not available) indicated an area of convergence oriented from northeast to southwest extending from a pendant at the southern tip of the northern line segment. (The radar beam at 0.2 degrees was sampling the storm at an elevation of around 250 m AGL at this time.) The inbound velocities associated with the convergence to the rear of the linear segment are coincident with a channel of minimum reflectivity, suggesting a subsident component to the flow.
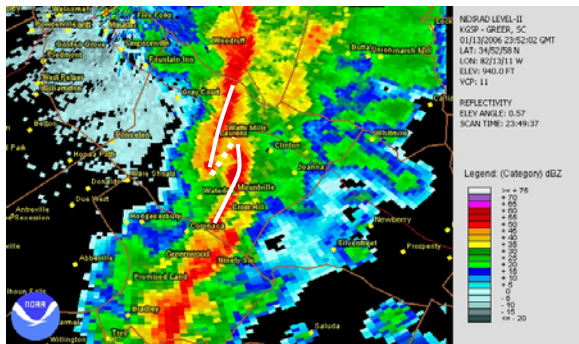

Figure 4. Reflectivity image at 0.5 degrees from the Greer, SC WSR-88D (KGSP) at 2352 UTC on 13 January 2006. The white lines trace the "broken-S" signature.

By 0105 UTC, a "broken-S" signature was evident approximately 6 km southwest of Bessemer City (Fig. 8), as the southern segment continued to move northeast slightly faster than the northern segment. However, there is a noticeable difference between the reflectivity pattern in Fig. 8 and that in Fig. 4. The "broken-S" pattern in Fig. 4 is quite distinct and very similar to what has been documented in previous studies. In these cases, the high reflectivity (>50 dBz) associated with the southern line segment extended north and east of the southern tip of the northern segment. This structure is not as evident in Fig 8.

There was a hint of cyclonic curvature in the reflectivity field at 0105 UTC within the southern tip of the northern segment. In addition, reflectivity continued to decrease within the channel of weak reflectivity between the two segments. Radial velocity (Fig. 9) indicated an area of low level convergence associated with

an apparent descending rear inflow jet extending southwest from the northern segment.
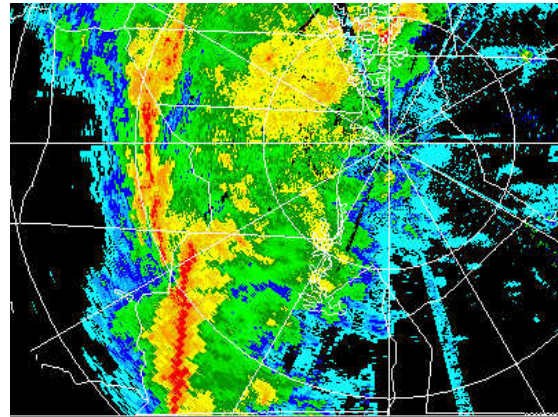

Figure 5. Base reflectivity image at 0.2 degrees from the Charlotte, NC TDWR (TCLT) at 0047 UTC on 14 January 2006.
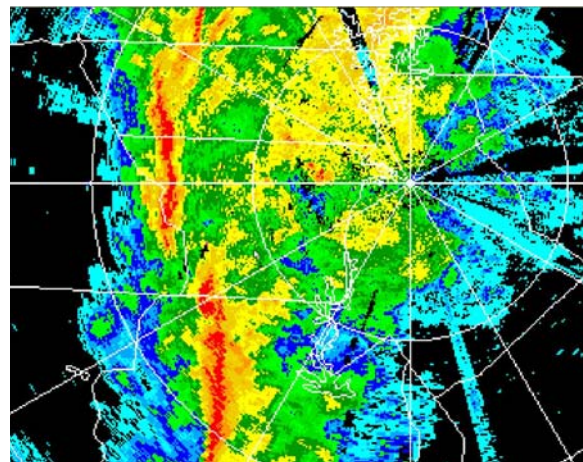

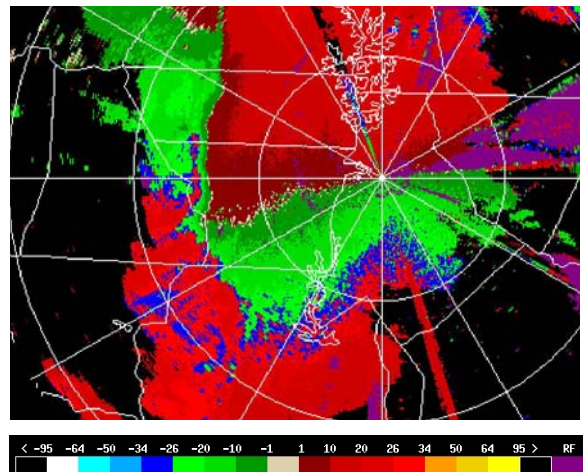**Figure 6. Same as in Fig. 5, except at 0059 UTC.**

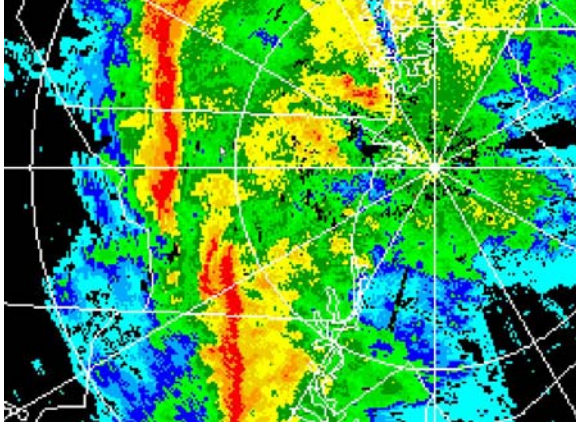**Figure 7. Radial velocity image from TCLT at 0059 UTC.**

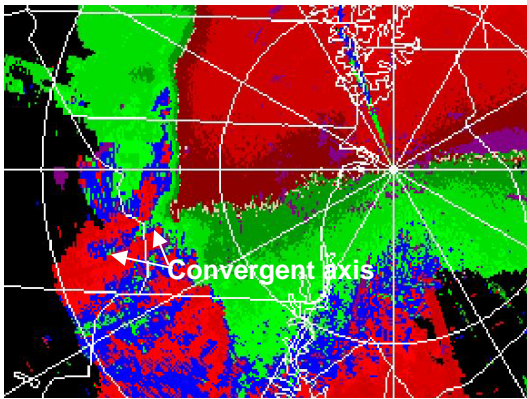**Figure 8. Same as in Fig. 5 except at 0105 UTC.**

Figure 9. Same as in Fig. 6, except at 0105 UTC.

The 0110 UTC TCLT scan (Fig. 10) was very near the time of tornado occurrence. The reflectivity data depicted a narrow pendant at the southern tip of the northern segment. A small indentation in the forward flank of this line segment was observed just north of the pendant. This was possibly indicative of an area of easterly storm-relative inflow. It is interesting to note that the reflectivity east of the pendant had decreased to < 20 dBz at this time. This suggests that the descending rear inflow jet apparent in the previous reflectivity images had turned cyclonically around the southern tip of the line segment. The radial velocity data continued to indicate a narrow band of outbound velocities extending southwest from the pendant. Coincident with the pendant, the velocity data revealed a weak rotational signature (Fig. 11). However, the data are difficult to interpret due to the absence of a storm relative velocity product. Subsequent images from TCLT actually depicted a hook-like appendage extending from the northern line segment (Fig. 12), although the significance of this is questionable, as the

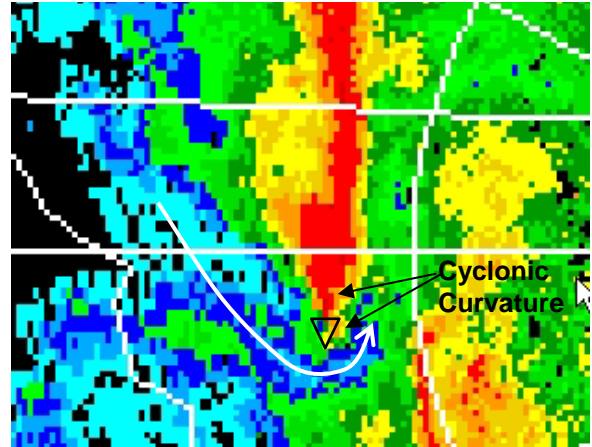feature was present several minutes after the tornado had dissipated.

Figure 10. Same as in Fig. 5 except at 0110 UTC. Tornado location is near the lower point of the triangle.
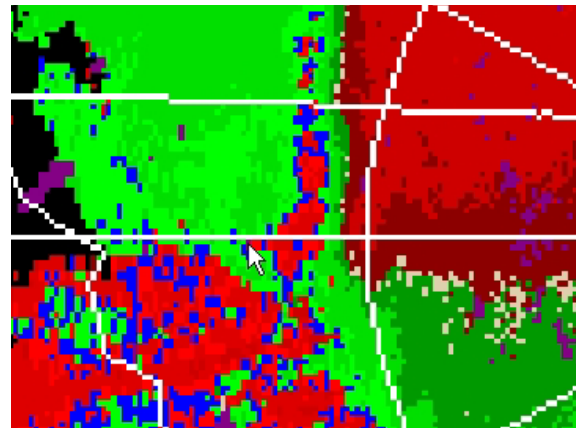

Figure 11. Same as in Fig. 6 except at 0110 UTC.

A series of images from KGSP prior to and during tornado occurrence (Figs. 13 and 14) reveal some significant differences with TCLT in regard to the detail of the structure of the evolving tornadic storm. Reflectivity images from KGSP did not reveal the cyclonic curvature in the images just prior to tornadogenesis. In addition, the forward flank inflow notch and the hook-like structure that were evident in the TCLT images from 0110 to 0112 UTC were absent in the KGSP reflectivity field. Although part of this can be attributed to the fact that KGSP is much farther away from the storm than TCLT, it can also be said that the higher resolution data provided by the 5-cm TDWR allows forecasters to see more detailed structure in precipitation systems.
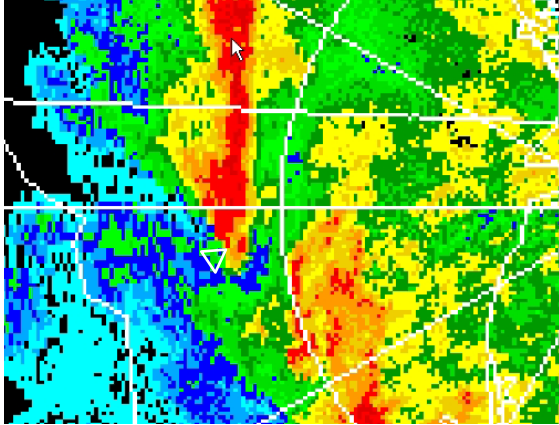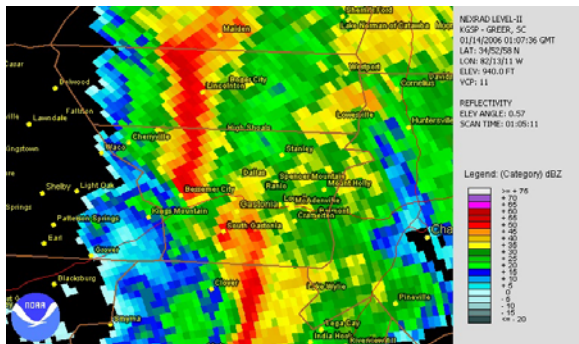
Figure 12. Same as in Fig. 5 except at 0112 UTC.

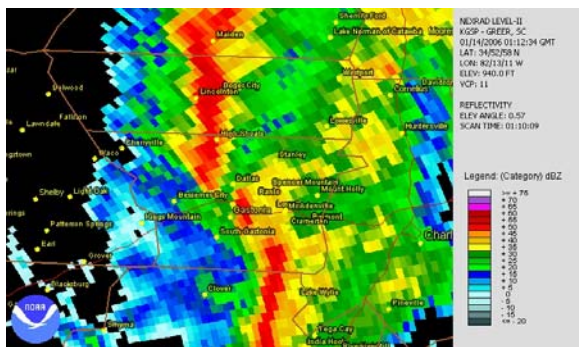**Figure 13. Same as in Fig. 4 except at 0107 UTC.**

Figure 14. Same as in Fig. 4 except at 0112 UTC.

4. DISCUSSION

The Bessemer City tornado of 13 January 2006 shared some of the radar characteristics of previous cool-season NST events studied in the eastern United States. However, there were some structural details that were somewhat unique to this event when compared to the "distinct broken-S" cases that have been previously documented. In the "distinct" cases, the following evolution is typically observed: 1) A region of high reflectivity (i.e., >50 dBz) within a

narrow, shallow QLCS exhibits a LEWP, 2) A narrow channel of weak reflectivity develops across the bowing segment, dividing the QLCS into two segments (northern and southern), with the northern extent of the southern segment typically positioned downstream of the southern tip of the northern segment (Fig. 4), and 3) The tornado occurs near the southern tip of the northern segment as the break develops, or shortly thereafter.

The BC tornado did not exactly follow this evolution. With the benefit of hindsight, one can argue that a break in the QLCS occurs after 0053 UTC (not shown). However, examination of reflectivity images prior to tornado occurrence reveals that the two high reflectivity segments that were later identified as constituting a "broken-S" pattern existed prior to the "break" in the line, with the apparent "break" occurring within an area of lower reflectivity between the two segments. This made pattern recognition difficult in real-time. In addition, the southern segment did not extend to the north and east of the northern segment. It is interesting to note that while several "typical" broken-S signatures were observed in radar data on this day, the BC event was the only tornado that occurred on 13 January 2006.

The rear-to-front, descending jet apparent in the BC storm appeared to play an important role in tornadogenesis. The numerical modeling studies of Weisman and Trapp (2003a,b) suggest that the source of intense, low-level rotation in QLCSs is through downward tilting of environmental, *crosswise* vorticity by sinking air currents, including the rear-inflow jet associated with organized mesoscale convective systems. Since this is the case, the amount of environmental, storm relative helicity may be inconsequential to non-supercell tornado occurrence, because it is a measure of the magnitude of streamwise vorticity. The magnitude of the vertical shear is a more accurate measure of the potential for NSTs. QLCSs modeled by Weisman and Trapp (2003) depicted development of strong low-level mesovortices with 0-2.5 km shear values of 20 m s^{-1}. The magnitude of the 0-2.5 km shear vector calculated from the sounding in Fig. 3 is approximately 26.1 m s^{-1}.

5. CONCLUSION

Detection of non-supercell tornadoes is one of the most difficult challenges facing operational

forecasters, especially in low CAPE environments. This is due to the fact that the mechanisms responsible for non-supercell tornadogenesis are obviously much different from that of supercell tornadoes. NSTs are not associated with deep, persistent mesocyclones and develop more rapidly than what is suggested by the "top-down" cascade associated with supercell tornadoes. Due to the small nature of NSTs, their circulations are almost always too small to be resolved by the radar beam. Only in the strongest cases is tornadogenesis preceded by an intense circulation in radar velocity data. Even in these cases, radar-indicated rotation will likely be detected only within several thousand feet of the ground and will precede tornadogenesis only by a matter of a few minutes, if at all.

Therefore, reliance upon Doppler velocity data in warning decision making may result in low probabilities of detection. Recognizing environments that are favorable for NSTs and radar reflectivity pattern recognition are the best tools for issuing effective warnings. Environments characterized by very strong low-level shear (0-3 km shear magnitude of 20 m s^{-1} or higher), low CAPE, and strong, linear forcing are favorable for development of shallow, narrow QLCSs and NSTs. Although forecasters may have a tendency to evaluate storm relative helicity in determining the tornadic potential in low CAPE environments, the magnitude of the low level shear may be of more importance in determining the NST potential. The presence of mid-level drying should further heighten forecaster awareness of the NST potential. Once this type of environment is recognized, it is best that forecasters go into a potential NST episode having already decided to issue a tornado warning if the "broken-S" signature is observed in reflectivity data. There is no utility in "waiting for the next volume scan" from the WSR-88D, as the tornado event, if it occurs, will likely have gone through its entire life cycle by the time data from the next volume scan are received. However, for forecasters with access to data from a TDWR, the 1-minute volume scan strategy increases the potential for issuance of timely warnings.

7. REFERENCES

Curtis, L., 2004: Midlevel dry intrusions as a factor in tornado outbreaks associated with landfalling tropical cyclones from the Atlantic and Gulf of Mexico. *Wea. Forecasting*, **19**, 411-427.

Grumm, R. H., and M. Glazewski, 2004: Thunderstorm types associated with the "broken-S" radar signature. Preprints, 22nd Conf. on Severe Local Storms, Hyannis, MA, Amer. Meteor. Soc., CD-Rom, P7.1.

Lee, L. G., and W. A. Jones, 1998: Characteristics of WSR-88D velocity and reflectivity patterns associated with a cold season non-supercell tornado in Upstate South Carolina. Preprints, 19th Conf. on Severe Local Storms, Minneapolis, MN, Amer. Meteor. Soc., 151- 154.

McAvoy, B. P., W. A. Jones, and P. D. Moore, 2000: Investigation of an unusual storm structure associated with weak to occasionally strong tornadoes over the Eastern United States. Preprints, 20th Conf. on Severe Local Storms, Orlando, FL, Amer. Meteor. Soc., 182-185.

Thompson, R. L., R. Edwards, J. A. Hart, K. L. Elmore, and P. Markowski, 2003: Close proximity soundings within supercell environments obtained from the Rapid Update Cycle. *Wea. Forecasting*, **18**, 1243-1261.

Weisman, M. L., and R. J. Trapp, 2003a: Low-level mesovortices within squall lines and bow echoes. Part I: Overview and dependence on environmental shear. *Mon. Wea. Rev.*, **131**, 2779-2803.

Weisman, M. L., and R. J. Trapp, 2003b: Low-level mesovortices within squall lines and bow echoes. Part II: Their genesis and implications. *Mon. Wea. Rev.*, **131**, 2804-2823.